Small angle x-ray scattering of chromatin

Radius and mass per unit length depend on linker length

Shawn P. Williams and John P. Langmore
Biophysics Research Division and Department of Biological Sciences, University of Michigan, Ann Arbor, Michigan 48109-2099 USA

ABSTRACT Analyses of low angle x-ray scattering from chromatin, isolated by identical procedures but from different species, indicate that fiber diameter and number of nucleosomes per unit length increase with the amount of nucleosome linker DNA. Experiments were conducted at physiological ionic strength to obtain parameters reflecting the structure most likely present in living cells. Guinier analyses were performed on scattering from solutions of soluble chromatin from *Necturus maculosus* erythrocytes (linker length 48 bp), chicken erythrocytes (linker length 64 bp), and *Thyone briareus* sperm (linker length 87 bp). The results were extrapolated to infinite dilution to eliminate interparticle contributions to the scattering. Cross-sectional radii of gyration were found to be 10.9 ± 0.5, 12.1 ± 0.4, and 15.9 ± 0.5 nm for *Necturus*, chicken, and *Thyone* chromatin, respectively, which are consistent with fiber diameters of 30.8, 34.2, and 45.0 nm. Mass per unit lengths were found to be 6.9 ± 0.5, 8.3 ± 0.6, and 11.8 ± 1.4 nucleosomes per 10 nm for *Necturus*, chicken, and *Thyone* chromatin, respectively. The geometrical consequences of the experimental mass per unit lengths and radii of gyration are consistent with a conserved interaction among nucleosomes. Cross-linking agents were found to have little effect on fiber external geometry, but significant effect on internal structure. The absolute values of fiber diameter and mass per unit length, and their dependencies upon linker length agree with the predictions of the double-helical crossed-linker model. A compilation of all published x-ray scattering data from the last decade indicates that the relationship between chromatin structure and linker length is consistent with data obtained by other investigators.

INTRODUCTION

Chromatin is the complex of DNA and protein which facilitates the storage and expression of genetic information in all plants and animals. The subunit of chromatin is the nucleosome, which is composed of a highly conserved core particle, one copy of the tissue-specific histone H1, and a tissue-specific amount of linker DNA. The primary structure of chromatin is a linear arrangement of nucleosomes along the DNA. Under phyiological salt conditions, the secondary structure of chromatin is the three-dimensional arrangement of the nucleosomes into a 25–40 nm diam fiber (reviewed by van Holde, 1989). Although the nucleosome core particle is known to near-atomic resolution (Richmond et al., 1984) the packing symmetry and connectivity of nucleosomes within the chromatin fiber are unresolved.

There is an abundance of models describing possible arrangements of nucleosomes within the chromatin fiber. These models can be separated into classes that are distinguished by their relationship between primary and secondary chromatin structure. Solenoid models (Finch and Klug, 1976; McGhee et al., 1983; Butler, 1984) have been proposed, which predict chromatin fiber diameters and mass per unit lengths that are independent of the linker length. Twisted-ribbon models (Worcel et al., 1981; Woodcock et al., 1984) predict diameters that have little or no linker length dependence, and mass per unit lengths that are inversely proportional to linker length. Crossed-linker models (Staynov, 1983; Makarov et al., 1985; Williams et al., 1986; Bordas et al., 1986*b*) predict a strong dependence of fiber diameter and mass per unit length upon the linker length. The models for chromatin structure have been extensively tested by many techniques including electron microscopy (e.g., Finch and Klug, 1976; Thoma et al., 1979; Woodcock et al., 1984; Williams et al., 1986), dichroism (e.g., McGhee et al., 1983; Makarov et al., 1985; Sen and Crothers, 1986; Dimitrov et al., 1988), and sedimentation velocity (e.g., Bates et al., 1981; Butler and Thomas, 1980; Pearson et al., 1983; Zentgraf and Franke, 1984; Thomas et al., 1986). Unfortunately none of these techniques has provided sufficient evidence to determine the structure. However, specific predictions of the models can be tested against the experimental data in hopes of eliminating some of the models from further consideration.

Low angle scattering from solutions of chromatin provides a model independent means for characterizing fiber morphology and for testing the predicted relationship between secondary structure and linker length. Salamander erythrocyte chromatin (*Necturus maculosus*, 48 base pair linker) and sea cucumber sperm chromatin

Address correspondence to Dr. Langmore.

0006-3495/91/03/606/13 $2.00

(*Thyone briareus,* 87 base pair linker) were chosen for the study because of the large difference in the linker lengths. Additionally, the decreased width and increased contrast of low angle scattering features suggested that the chromatin from these tissues would be well ordered and amenable to electron microscopic investigation (Williams et al., 1986). Chicken erythrocyte chromatin (*Gallus domesticus,* 64 base pair linker) was chosen as an intermediate linker tissue because it is a standard for chromatin structural analysis, although less ordered than the other tissues examined (Williams et al., 1986). Under ideal conditions Guinier analysis of the scattering is a model-independent method to determine the cross-sectional radius of gyration (R_c) and mass per unit length (M_1) of the isolated fibers. Measurements of R_c and M_1 were made at different chromatin concentrations and the results extrapolated to infinite dilution to eliminate interparticle contributions to the scattering. The results of these studies were compared with those of the last decade of x-ray studies of chromatin.

Measurements were made at physiological salt concentration to reflect the structure most likely present in cells under native conditions, and to relate the results to diffraction features observed previously in nuclei and living cells (Langmore and Schutt, 1980; Langmore and Paulson, 1983; Williams et al., 1986). Measurements were performed over a concentration range of 50–300 μg/ml to relate the results to previous electron microscopic and hydrodynamic studies. Past x-ray scattering studies have been performed with chromatin that had been concentrated to 2.5–50 mg/ml and over a range of ionic conditions. Many procedures exposed the chromatin to dialysis or sedimentation; procedures that we found cause extensive loss of H1. As a further control for electron microscopic and sedimentation analyses, the effects of glutaraldehyde and formaldehyde fixation on fiber structure were investigated.

MATERIALS AND METHODS

Buffers

Wash buffer (WB) consisted of 130 mM NaCl, 5.0 mM KCl, 2.0 mM $MgCl_2$, 10 mM Hepes (pH 7.0), and 0.1 M sucrose. Synthetic Sea Water (SSW) was prepared from a powder obtained from Instant Ocean (East Lake, OH). Buffer A contained 60 mM KCl, 15 mM NaCl, 15 mM PIPES (pH 7.0), 0.5 mM spermine, 0.5 mM spermidine, 2.0 mM EDTA, 0.02% NaN_3. Buffer EB contained 60 mM KCl, 15 mM NaCl, 15 mM PIPES (pH 7.0), 3.0 mM EDTA, 0.1 mM PMSF, and 0.02% NaN_3. Micrococcal nuclease digestion buffer (MNase DB) was the same as EB except EDTA was replaced by 0.5 mM $CaCl_2$ and 0.25 mM $MgCl_2$. Buffer MB was the same as EB except 3.0 mM $MgCl_2$ replaced EDTA.

Isolation of nuclei

Erythrocytes from Long Island White chickens (Dave's Eggs, MI), or *Necturus maculosus* (Charles Sullivan, TN) were obtained by heart puncture. Sperm from *Thyone briareus* (Woods Hole Marine Biological, MA) were obtained in sea water from minced gonads. All subsequent steps were performed at 4°C, and all washes were to volumes at least 10 times that of the pellet. Except where noted, *Necturus* erythrocytes and nuclei were centrifuged for 6 min at 50 *g*, and chicken erythrocytes and nuclei were centrifuged for 10 min at 290 *g* during the washing steps. Erythrocytes were washed two times in WB, with the buffy coat removed to eliminate lymphocytes. The erythrocytes were then incubated for 1 h on ice in WB with 3 mM iodoacetate, and 0.2 mM PMSF to inhibit proteases. Living sperm were washed two times in SSW (20 min at 800 *g*) and were then incubated for 1 h on ice in buffer A and 1 M sucrose, 3 mM iodoacetate, and 0.2 mM PMSF. *Thyone* sperm were then pelleted for 10 min at 200 *g*. Subsequent steps were very similar for the three tissues. Cells were washed three times in buffer A with 0.1% digitonin, 1 mM iodoacetate, and 0.1 mM PMSF, and three times buffer A with 0.1% Non-idet P40, 1 mM iodoacetate, and 0.1 mM PMSF. Nuclei were resuspended to 1 mg/ml in buffer A with 50% glycerol and quickly frozen by placing 1 ml aliquots within Eppendorf centrifuge tubes into a solution of methanol/dry ice. Nuclei were stored at −70°C.

Isolation of chromatin

All steps were carried out in 1 ml volumes. *Necturus* were always centrifuged for 6 min at 50 *g*; chicken and *Thyone* for 10 min at 180 *g*. One mg aliquots of nuclei were pelleted at 4°C, resuspended in MB, and then washed with MNase DB. Nuclei were then resuspended in MNase DB and incubated at 22°C for 5 min. Nuclei were digested with 20 units micrococcal nuclease (Worthington) for 3 (*Thyone*), 4 (chicken), or 5 (*Necturus*) min, to solubilize chromatin of comparable molecular weights. Digestion was stopped by addition of EGTA to 5.0 mM and $MgCl_2$ to 1.0 mM. Nuclei were then pelleted and resuspended in 5.0 mM EDTA pH 7.0, 0.1 mM PMSF to solubilize chromatin. Nuclei were allowed to lyse at 4°C for 30 min to 1 h, and then spun for 10 min in an Eppendorf centrifuge to pellet debris. Yields were 10–15% for *Thyone,* and 15–20% for *Necturus* and chicken. The oligomers obtained by such a procedure are up to 150 nucleosomes long. Chromatin is brought to physiological ionic strength by adding one-tenth volume 10 × EB. In the case of *Necturus* and *Thyone,* the average nucleosome repeat length of the solubilized chromatin was determined to be the same as that of the bulk nuclei.

Calibration standards

Tobacco mosaic virus (TMV) was a generous gift of Drs. T. Schuster and R. Raghavandra, and was examined in EB. F-actin was a gift of Dr. S. Brown, and was studied in 0.1 M KCl, 1 mM $MgCl_2$, 1 mM ATP.

Sample evaluation

Proteins were assayed after data collection by SDS PAGE in 15% polyacrylamide gels. Proteins were visualized using equilibrium Coomassie staining (Neuhoff et al., 1988). Accurate quantitation of histones required direct densitometry. Transmitted light was recorded using a SONY XC77 CCD camera attached to an ITI FG100 acquisition board (Imaging Technology Inc., MA) in a VAXstation 3500. Images were acquired and averaged using the program GETPIC written for the VAX in the C programming language. The transmitted intensities were converted to optical densities and interactively analyzed on a Silicon Graphics 2500T using the FORTRAN program

TOTAL2. Individual lanes were boxed off and projected perpendicular to the lane axis for peak integration. Intensities of pixels at the box edges were used for background subtraction.

DNA was isolated from chromatin by digesting samples for 2–4 h at 45°C with 1 μg/ml Proteinase K in 1% SDS. DNA fragments were separated according to size by running a 0.3% agaros gel at 1 V/cm for 36 h. The amount of DNA was quantitated by digitizing the fluorescence of ethidium bromide stained gels illuminated from below with UV light. The distribution of DNA lengths was estimated from DNA mobility relative to that of molecular weight standards (e.g., High Molecular Weight Standards [BRL, MD], and oligomers of phage λ DNA).

Collection of scattering data

Data were collected on an Elliot GX-20 rotating anode with a double mirror Franks camera and a linear position sensitive detector described previously (Langmore and Paulson, 1983). Spectra were collected with a specimen to detector distance of 1.4 m and a resolution of 0.1 mrad. Data were collected until 1% statistics were achieved at $s = 0.025$ nm^{-1} ($s = 2\sin\theta/\lambda$, where θ = the Bragg angle and $\lambda = 0.154$ nm). A chromatin concentration of 0.2 mg/ml required an exposure time of $\sim 2 \times 10^5$ s. Samples were kept at 4°C during the exposure in scattering chambers consisting of ⅛-in thick Plexiglass sample holders with Kapton windows. Chamber thicknesses were measured by beam absorbance, and were found to vary by <5%. Sample holders were sealed with Vaseline to prevent evaporation. After x-ray exposure, samples were examined by electron microscopy and SDS PAGE to determine structural integrity. All scattering studies employed unfixed samples in EB unless otherwise noted.

Processing of low angle spectra

The initial step in analysis was the subtraction of instrumental and cosmic ray background. Specra were then folded about their centers of symmetry to increase the signal-to-noise ratio. Integrated beam intensity was normalized using the assumption that scattering at $s > 0.2$ nm^{-1} was due exclusively to solvent scattering at the very low chromatin concentrations. Solvent spectra were subtracted after scaling.

The data were deconvoluted to correct for experimental beam profile and detector slit height, using a reciprocal space iterative algorithm (Lake, 1967). The algorithm was tested by correcting theoretical spectra that had been intentionally convoluted by the experimental collection geometry, and was found to be accurate to 2%. Measured values of the cross-sectional radius of gyration (R_c) obtained from f-actin were completely unaffected by deconvolution. However, deconvolution was necessary to determine R_c from larger particles, such as TMV and chromatin. Uncorrected TMV data gave an R_c of 5.9 nm, whereas the deconvoluted data gave an R_c of 6.5 nm. The actual value of R_c was determined to be 6.4 nm using the two-dimensional detector at the Brookhaven High Flux Beam Reactor, demonstrating the accuracy of these procedures. Deconvolution of the chromatin data corrected R_c by <15%.

Radius of gyration analysis

The cross-sectional radii of gyration, R_c, were calculated from the deconvoluted data by plotting ln(kI) vs. k^2, where $k = 2\pi s$ (Guinier and Fournet, 1955; Luzatti, 1960; Kratky, 1964), yielding a slope equal to $-2.0R_c$. R_c is related to the radius of a solid cylinder by the equation $R = 2\sqrt{2}\,R_c$. The angular region used for Guinier analysis was s = 0.015–0.036 nm^{-1}. Slopes and intercepts obtained from Guinier plots were insensitive to the exact angular region chosen within this interval. Portions of the scattering curves were used that gave a best least squares fit to straight lines, as judged by lowest chi square and correlation coefficient closest to −1.0.

Mass per unit length analysis

Mass per unit length, M_1, of isolated fibers was obtained by comparing the extrapolated zero angle scattering of chromatin solutions to that from TMV solutions of known concentration. The equation which relates M_1 to scattering intensity of different samples is (Greulich et al., 1987):

$$M_{lch} = M_{lstd} \times \frac{I(0)_{ch} C_{std} \left(\frac{\partial \rho_{el}}{\partial C}\right)^2_{std}}{I(0)_{std} C_{ch} \left(\frac{\partial \rho_{el}}{\partial C}\right)^2_{ch}}, \quad (1)$$

where $(\partial\rho_{el}/\partial C) = l_1 - l_2\nu_2\rho_1$, and: M_{lch} = mass per unit length of the chromatin fibers, M_{lstd} = mass per unit length of the standards, $I(0)_{ch}$ = normalized zero angle scattering of the chromatin solution, $I(0)_{std}$ = normalized zero angle scattering of the standard solution, C_{ch} = mass concentration of the chromatin solution, C_{std} = mass concentration of the standard solution, $\partial\rho_{el}/\partial C$ = change in excess electron density per mass concentration of solute, l_1 = number of electrons per gram of solution, l_2 = number of electrons per gram of solute, ν_2 = partial specific volume of solute, and ρ_1 = density of the solution.

Based on electron/mass ratios of 0.334, 0.325, and 0.309×10^{24} e$^-$/g for H_2O, histone, and sodium DNA respectively (Greulich et al., 1985) the excess electron densities of chromatin and TMV could be calculated once the protein:DNA ratio was known. Relative proportions of histone and DNA were estimated from the linker lengths of *Necturus*, chicken, and *Thyone*, and on the histone molecular weights. Partial specific volumes of histone and sodium DNA were taken to be 0.75 and 0.56 cm^3/g, yielding partial specific volumes of 0.655, 0.652, and 0.646 cm^3/g for *Necturus*, chicken, and *Thyone* chromatin, in agreement with measured values in 0.1 M NaCl (Koch et al., 1987). The above figures lead to excess electron densities of 0.098, 0.099, and 0.100×10^{24} e$^-$/g for *Necturus*, chicken, and *Thyone* chromatin, respectively. Excess electron density of TMV was estimated from the known protein and RNA content (Markham et al., 1964) to be 0.077×10^{24} e$^-$/g. TMV was assumed to have an M_1 of 131 kDa/nm (Caspar, 1963). After x-ray exposure chromatin concentrations were measured by A_{260} on a Perkin-Elmer Lambda 4C spectrophotometer, assuming $A_{260} = 1.0$ for 50 μg/ml DNA. TMV concentration was calculated assuming $A_{260} = 3.06$ for 1 mg/ml TMV (Boedtker and Simmons, 1958).

Fixation of nuclei and chromatin

Nuclei from *Necturus* erythrocytes and *Thyone* sperm were washed extensively in EB and cross-linked with either 0.1% or 1% glutaraldehyde, or 1% formaldehyde for 13 h at 4°C. Nuclei were then washed three times with EB to remove excess fixative. Nuclei were loaded into glass capillaries and centrifuged into a concentrated pellet to obtain the highest sample concentration. Pellet volumes of all cross-linked nuclei were substantially larger than noncross-linked samples, showing an overall resistance to compaction. Isolated chromatin was fixed with 0.1% or 1% glutaraldehyde for 13 h and then dialyzed against EB.

RESULTS

Histone molecular weights for *Necturus* and *Thyone*

Molecular weights of *Necturus* and *Thyone* histones were used to determine the protein/DNA ratio and nucleosome mass, which were needed to determine M_1. Histone molecular weights were calibrated using a least squares fit of chicken erythrocyte histone SDS-PAGE mobilities and molecular weights (van Holde, 1989). Table 1 shows the molecular weights of *Necturus* and *Thyone* histones calculated from SDS-PAGE mobilities (Fig. 1). Assuming two copies each of H4, H3, H2A, and H2B, and one copy of H1 (or H5) per nucleosome, the nucleosome molecular weights are 259, 270, and 282 kDa, and histone/DNA mass ratios are 1.0, 0.93, and 0.82 for *Necturus,* chicken, and *Thyone,* respectively. These values are subject to the uncertainties in histone stoichiometry, especially those of H1 and H5 (van Holde, 1989).

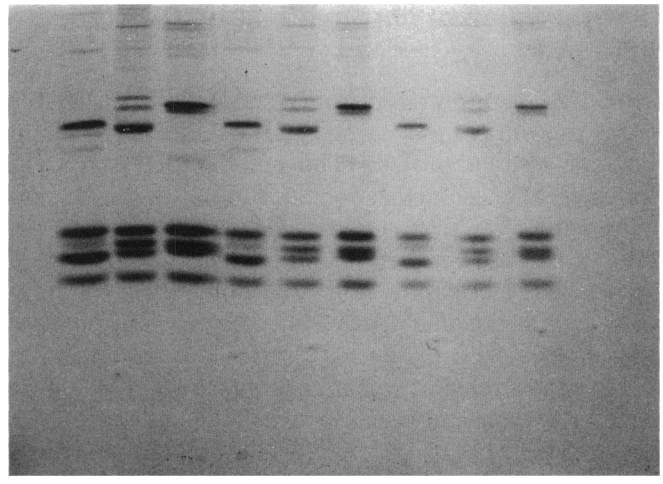

FIGURE 1 SDS-Polyacrylamide gel electrophoresis of histones: (lanes 1, 4, 7) *Thyone;* (lanes 2, 5, 8) chicken; (lanes 3, 6 9) *Necturus;* at 2.0, 1.0, and 0.5 μg protein per lane.

Maintenance of H1 content

It was necessary to determine isolation conditions that best preserved the native histone composition. The H1 to core histone ratio of *Thyone* chromatin isolated by different procedures was compared with sperm nuclei by densitometric analysis of Coomassie stained polyacrylamide gels (Fig. 2). Measurements were reproducible to 5%. Comparison of integrated H1 histone bands to core histone bands shows that chromatin isolated by lysing the nuclei in 5 mM EDTA maintains 94% of the original amount of H1, which decreases to 79% after dialysis against EB. When the chromatin is obtained by lysis at higher ionic strength, only 61% of H1 is retained, which decreases to 57% after dialysis against EB. In contrast, visual inspection of the gels gives the impression that the H1 content is unchanged, regardless of treatment. When chromatin isolated at 5 mM EDTA is added to one-tenth volume 10 × EB rather than subjected to dialysis, the measured H1 ratio is indistinguishable from nuclei. To measure the amount of H1 bound to these fibers, the high molecular weight chromatin was pelleted in a Beckman Airfuge. The ratio of H1 to core histones was 95% of that found in nuclei. Thus, a low ionic strength lysis and direct adjustment of ionic strength is expected to maintain native higher order structure better than lysis or dialysis in EB, which cause H1 loss.

TABLE 1 **Molecular weights of *Necturus*, chicken, and *Thyone* histones**

Histone	Mol. weight (*kDa*)		
	Necturus	chicken*	*Thyone*
H4	11.8 ± 0.2	11.2	12.0 ± 0.2
H2A/B	13.8 ± 0.2	13.8	13.2 ± 0.2
H3	14.6 ± 0.2	15.3	14.6 ± 0.2
H1	21.7 ± 0.2	21.9	20.8 ± 0.2

*Taken from Wang et al. (1985), using H5 to calibrate H1.

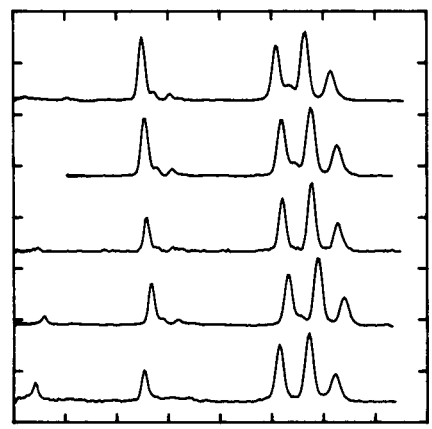

FIGURE 2 Densitometric scans of Coomassie-stained *Thyone* chromatin proteins. Large peak on left is H1; peaks on right are core histones. From top to bottom: nuclei in MNase DB; chromatin after 5 mM EDTA lysis; chromatin after EB lysis; chromatin after 5 mM EDTA lysis and dialysis; chromatin after EB lysis and dialysis.

Preservation of chromatin fiber integrity

Solutions were removed from sample holders after the x-ray exposures and assayed by SDS-PAGE to check for loss of histone protein. The amount of histone H1 present after solubilization and x-ray exposure was surprisingly variable. A correlation existed between the amount of H1 present and the measured radius of gyration. For example, a 40% deficiency of H1 results in a 15% reduction in R_c. Scattering data were not analyzed if less than 80% of the nuclear H1 was present after x-ray exposure. Electron micrographs of samples were similar to those published earlier (Williams et al., 1986; Athey et al., 1990). Micrographs of samples before and after the x-ray exposures could not be distinguished.

Low-angle x-ray scattering from a pellet of isolated chromatin fibers in EB gave rise to the same high angle diffraction features obtained from pellets of isolated cell nuclei (Fig. 3), indicating preservation of the internal structure of chromatin during the isolation process.

Validity of Guinier analysis

An important assumption for the validity of the modified Guinier analysis is that the fibers are adequately long. Fig. 4 shows the results of applying Guinier analysis to the formula for low angle scattering from solid cylinders of finite length (Guinier and Fournet, 1955; Malmon, 1957). If the axial ratio is greater than two the measured values for R_c and M_1 will be >90% of the values obtained for infinitely long fibers. DNA gels indicated

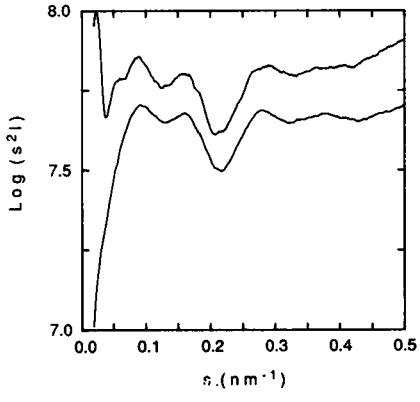

FIGURE 3 Low-angle scattering patterns from *Necturus* nuclei (*top*) and chromatin (*bottom*). Chromatin was concentrated by sequential dialysis against 60% sucrose 5 mM EDTA, and then 5 mM EDTA alone before precipitation by addition of one-ninth volume of 10 X EB. The chromatin pellet was extremely condensed as exhibited by both the lack of scattered intensity at low angles, and the good resolution of the higher angle features.

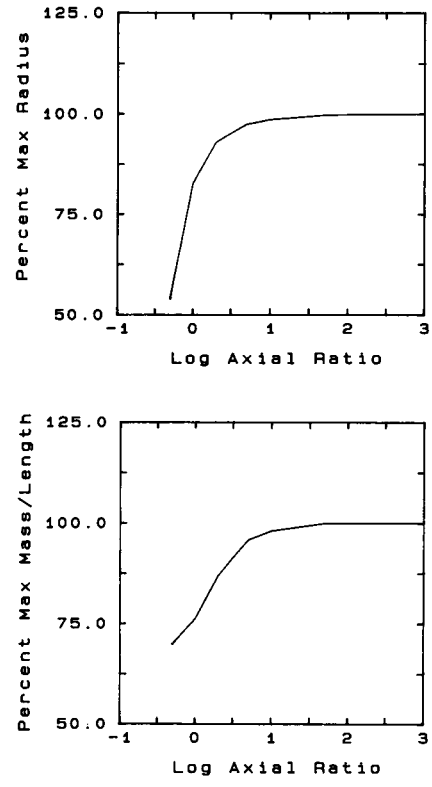

FIGURE 4 Calculated effects of finite fiber length on measured parameters. (*a*) Measured R_c relative to the maximum radius of gyration, which is from a fiber of infinite length. (*b*) Measured M_l relative to the maximum mass per unit length, which is from a fiber of infinite length.

mass average sizes of 196, 153, and 134 nucleosomes for the samples of *Necturus,* chicken, and *Thyone,* respectively. Using the measurements for M_l and fiber radius from the scanning transmission electron microscope (STEM) (Woodcock et al., 1984; Williams et al., 1986), the estimated axial ratios for the *Necturus,* chicken, and *Thyone* fibers used in this study are 9.6, 5.8, and 2.8, respectively. As a control, a *Thyone* sample with two-thirds the molecular weight was also measured and gave results indistinguishable from the higher molecular weight specimens. These results validate the Guinier analysis.

Radii of gyration

To check the accuracy of our measurement techniques, R_c of f-actin and TMV were measured and found to be 2.6 and 6.4 nm. The value for f-actin agrees well with the 2.57 nm measured previously (Hartt and Mendelson, 1980). The value for TMV agrees with that expected for

a 18 nm diam cylinder with a 4 nm hole, and with STEM measurements (Smith et al., 1990).

Guinier analysis was performed on chromatin isolated from *Necturus,* chicken, and *Thyone* chromatin. The excellent linearity of the Guinier plots (Fig. 5) is a measure of the statistical significance of the data and the ideality of the chromatin solutions. Data were collected at several chromatin concentrations for each cell type, and values obtained from analyzing the spectra were extrapolated to zero concentration to exclude effects of solution nonideality (Fig. 6). Values of 10.9 ± 0.5, 12.1 ± 0.4, and 15.9 ± 0.5 nm were obtained for R_c of isolated *Necturus* erythrocyte, chicken erythrocyte, and *Thyone* sperm chromatin. The small concentration dependence of R_c indicates that the solutions were nearly ideal. Assuming that the solutions were perfectly ideal, the estimated values of R_c would be the average of all the measurements, namely 11.7 ±0.3, 12.4 ± 0.4, and 15.5 ± 0.3 for *Necturus,* chicken, and *Thyone* chromatin. Thus there was little evidence for aggregation. This result has been found for other types of chromatin. Thus there was little evidence for aggregation. This result has been found for other types of chromatin at much higher concentrations (e.g., Suau et al., 1979; Gerchman and Ramakrishnan, 1987; Greulich et al., 1987; Koch et al., 1988).

Mass per unit length

Given the observed variation in chromatin fiber diameter with linker length, it was of interest to determine whether the packing density of nucleosomes within chromatin secondary structure is constant. Measured scattering from chromatin solutions was extrapolated to zero concentration to determine values appropriate to single particle scattering, and normalized using the zero-angle scattering relative to solutions of TMV of known concentration (Fig. 7). The experimental values of M_l did not show a significant dependence upon concentration. The M_l values extrapolated to infinite dilution were 180 ± 12, 225 ± 17, and 333 ± 39 kDa/nm for *Necturus,* chicken, and *Thyone* chromatin, respectively. Division of M_l by the experimental nucleosome masses yielded 6.9 ± 0.5, 8.3 ± 0.6, and 11.8 ± 1.4 nucleosomes per 10 nm for *Necturus,* chicken, and *Thyone* chromatin, respectively. Assuming that the solutions were perfectly ideal (i.e., that the actual value of M_l did not depend at all upon concentration, the estimated values of M_l would be 6.1 ± 1.4, 8.5 ± 0.57, and 11.9 ± 0.8 nucleosomes per 10 nm for *Necturus,* chicken, and *Thyone* chromatin).

The slopes of M_l vs. concentration plots reflect differences in the aggregation tendencies of TMV and isolated chromatin fibers. TMV scattering plotted in this fashion exhibited a positive slope, indicating the nonneg-

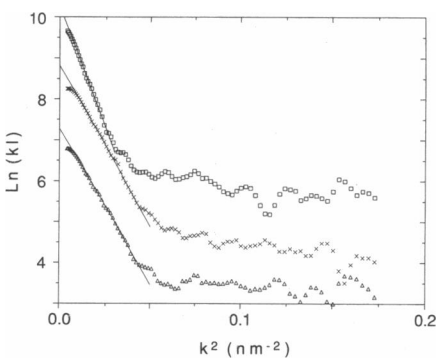

FIGURE 5 Representative Guinier plots showing the difference in R_c of chromatin from three tissues. Curves shown are (*from top to bottom*): *Thyone* sperm chromatin (160 μg/ml); chicken erythrocyte chromatin (130 μg/ml); and *Necturus* erythroctye chromatin (125 μg/ml). Data are not shown on an absolute scale, in order that the lines do not overlap.

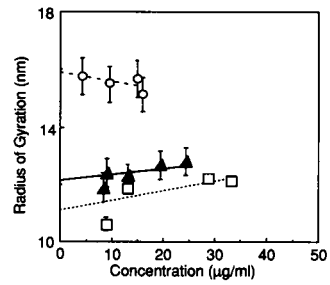

FIGURE 6 R_c as a function of concentration. (○) *Thyone;* (▲) chicken; and (□) *Necturus* chromatin. Lines shown are the results of least squares linear regression of R_c vs. concentration data for: (— —) *Thyone* sperm; (——) chicken erythrocyte; and (· · · ·) *Necturus* erythrocyte chromatin. The intercept is R_c at infinite dilution.

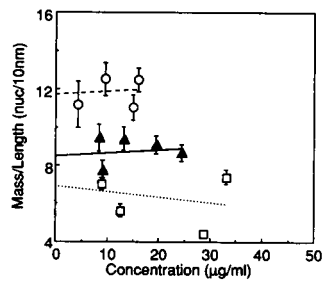

FIGURE 7 M_l as a function of concentration. (○) *Thyone;* (▲) chicken; and (□) *Necturus* chromatin. Lines shown are the results of least squares linear regression of M_l vs. concentration for: (— —) *Thyone* sperm; (——) chicken erythrocyte; and (· · · ·) *Necturus* erythrocyte chromatin. The intercept is M_l at infinite dilution.

ligible contributions of particle interactions to the measured scattering even at small concentrations. TMV is known to aggregate, and even forms domains with substantial alignment under more concentration conditions (Bernal and Fanchuchen, 1941). The extremely weak concentration dependence of the M_1 of the chromatin fibers shows that the chromatin used in this study had less tendency to aggregate than TMV.

Effects of fixation on chromatin fibers

Electron microscopic studies of isolated chromatin fibers require the samples to be cross-linked before examination to prevent denaturation on the carbon substrate or at the air-water interface (Dubochet et al., 1988). Low angle diffraction of all cross-linked nuclei showed a decrease in the scattering intensities at $s = 0.1$ nm^{-1} and $s = 0.16$ nm^{-1} relative to scattering from unfixed nuclei (Fig. 8), indicating that the internal structure of cross-linked fibers had less contrast or was less regular. Spectra did not exhibit the characteristic reflection at $s = 0.03$ nm^{-1} due to side-by-side packing of fibers in nuclei (Langmore and Schutt, 1980; Langmore and Paulson, 1983; Widom and Klug, 1985), indicating changes in the diffraction spectra were probably not due to fiber aggregation.

To assay possible changes in fiber geometry and mass per unit length due to fixation, Guinier analysis was performed on scattering from solutions of cross-linked isolated chromatin fibers. The measured R_c of unfixed, 1% and 0.1% glutaraldehyde fixed *Necturus* fibers isolated from the same preparation were 10.6, 11.6, and 11.6 nm, respectively. The measured M_1 of both 0.1% and 1% glutaraldehyde fixed *Necturus* fibers was 6.4 nuc/10 nm, compared with 7.0 nuc/10 nm for the unfixed sample. The measured R_c of unfixed, 0.1% and 1% glutaraldehyde fixed *Thyone* fibers isolated during the same preparation were 15.7, 15.4, and 16.1 nm, respectively. The measured M_1 of unfixed, 0.1% and 1% glutaraldehyde fixed *Thyone* fibers were 11.1, 12.3, and 15.3 nuc/10 nm, respectively. The straight Guinier plots indicated no aggregation.

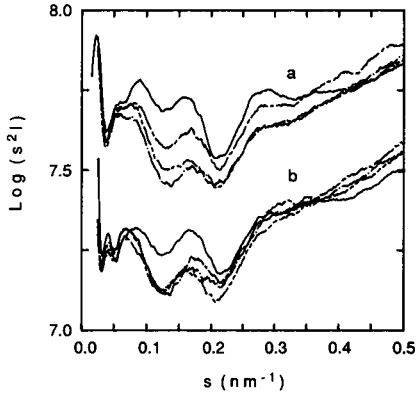

FIGURE 8 The effects of fixation upon internal structure of chromatin. The curves were positioned to superimpose the lowest angle scattering. (*a*) *Necturus* nuclei: (———) unfixed; (— — —) 0.1% glutaraldehyde fixed; (———) 1%) glutaraldehyde fixed; (———) 1% formaldehyde fixed. (*b*) *Thyone* nuclei: (———) unfixed; (— — —) 0.1% glutaraldehyde fixed; (———) 1% glutaraldehyde fixed; (———) 1% formaldehyde fixed.

DISCUSSION

Chromatin has been studied by x-ray scattering for many years. It has been difficult to make conclusions about the role of the internucleosomal DNA, because the dependence of the structure upon linker length had been masked by differences in isolation procedures, salt conditions, and analytical methods. Most previous studies had been made on fibers that were 3–10 times shorter than our fibers, and without quantitating retention of H1. In addition, the other studies were performed on chromatin that was 8–1,000 times more concentrated. We have studied three types of chromatin using identical techniques of isolated, data collection, and analysis. The absolute calibration of the results were checked by examination of f-actin and TMV. Table 2 summarizes these results, which can be compared to previous scattering, hydrodynamic, and microscopic studies. Our results agree with a number of recent studies indicating that the diameter and mass per unit length of chromatin fibers depend upon the length of linker DNA. These results are inconsistent with constant-diameter models, but are consistent with crossed-linker models for chromatin.

It has been known for a long time that H1 is required for the correct folding of chromatin (Thoma et al., 1979). Therefore, isolated chromatin containing the original complement of H1 is expected to have the highest probability of forming native higher order structure. Our results suggest that a low ionic strength lysis minimizes H1 loss compared with isolation procedures

TABLE 2 **Summary of measured structural parameters**

Chromatin	Linker length	R_c	Diameter	M_1
	bp	*nm*	*nm*	*nuc/10 nm*
Necturus	48	10.9 ± 0.5	30.8 ± 1.4	6.9 ± 0.4
Chicken	64	12.1 ± 0.4	34.2 ± 1.1	8.3 ± 0.6
Thyone	87	15.9 ± 0.6	45.0 ± 1.7	11.8 ± 1.0

using higher salt concentrations or dialysis. This loss of H1 during high ionic strength lysis is due to either a migration of the molecules to larger fibers retained in the nucleus (Thomas and Rees, 1983), or preferential solubilization of an H1-depleted subfraction. Loss of H1 during dialysis is presumably caused by small amounts of free H1 at higher ionic strength (Caron and Thomas, 1981) adhering to the dialysis tubing. A 40% loss of H1 was correlated with a 15% reduction in R_c, consistent with an unraveling of the structure. Thus, all measurements of chromatin are potentially limited by deficiencies or heterogeneities in H1 content.

The structural integrity of the very dilute chromatin solutions used in this study was confirmed by the facts that (*a*) ultracentrifugation found the native amount of H1 bound to the high molecular weight chromatin; (*b*) x-ray scattering from precipitated chromatin agreed with that from intact nuclei; and (*c*) electron microscopy and SDS-PAGE of chromatin after x-ray exposure showed no changes in structure. Our conclusion is that both x-ray scattering and electron microscopic studies are examining chromatin in the same structural state.

Chromatin fiber structure depends on linker length

Different models for chromatin can be distinguished on the basis of absolute fiber diameter and dependence of the diameter upon linker length. The results presented here (Table 2) clearly exhibit the correlation between R_c and the amount of DNA in the nucleosome. Fibers measured were of adequate axial ratio for application of Guinier analysis. Guinier plots exhibited straight lines indicating that samples were not aggregated. R_c was found to be virtually independent of chromatin concentration, another indication that solutions were behaving ideally. Although the uncertainties in the scattering measurements at very low concentrations made it more difficult to distinguish between the *Necturus* and chicken results, the diameter of *Thyone* chromatin was clearly larger than that of the shorter-linker tissues.

Chromatin mass per unit length increased with linker length (Table 2). The M_1 values were independent of concentration, demonstrating a lack of aggregation. Because R_c also depends upon linker length, there is a correlation between fiber diameter and M_1.

It has been asserted, without evidence, that the measured differences in chromatin diameters and mass per unit length were artifacts due to chromatin aggregation (Widom and Klug, 1985; Widom, 1989). Results presented here show that the differences exist in unaggregated chromatin in a physiological environment.

Effects of cross-linking agents on chromatin structure

Because electron microscope studies utilize cross-linking agents to stabilize chromatin, we were interested in the effects of fixation. Glutaraldehyde and formaldehyde fixation of nuclei caused a significant decrease and shift in the scattering maxima at $s = 0.1$ nm^{-1}, and at $s = 0.16$ nm^{-1}, signifying disturbance of the internal fiber structure.

R_c and M_1 of glutaraldehyde-fixed chromatin were measured to assay the effects of cross-linking on the external geometry. Because the observed differences in R_c were small, we conclude that fixation did not affect fiber diameter. These results agree with the observation that fixation does not affect the scattering from nuclei in the region of $s = 0.014$–0.05 nm^{-1}. Glutaraldehyde fixation of chromatin significantly increased the mass per unit length. In conjunction with the scattering from nuclei, the results indicate that although the external geometry of chromatin is unaffected by fixation, the internal structure is severely distorted. Even mild fixation with glutaraldehyde or formaldehyde should be avoided for high resolution studies of chromatin structure.

Comparison with previous low angle scattering studies

The relationship between R_c and linker length has been observed in other low-angle scattering studies. Fig. 9 is a compilation of low-angle scattering studies performed on isolated chromatin under conditions favoring higher order structure. A linear regression analysis of the dependence of the apparent diameter upon linker length yields an intercept of 22 nm and a slope of 0.19 nm/bp. The trend is most clearly exhibited in those studies where histone content was closely monitored, and fibers were of sufficient length for valid Guinier analysis. The trend is apparent with a variety of salt conditions and isolation techniques indicating that the relationship between fiber diameter and linker length is an intrinsic property of chromatin.

The large uncertainties in the measurements of R_c and M_1 shown in Fig. 9 exemplify the difficulties experienced with preparing samples and interpreting x-ray data. The measured value for chicken erythrocyte chromatin of $R_c = 12.1$ nm obtained in this study is in good agreement with the average value of 11.8 ± 1.6 nm obtained from the other studies. The lower values of 8.8 nm obtained by Greulich et al. (1987) and 9.5 nm obtained by Suau et al. (1979) might be indicative of unraveling of chromatin due to unmeasured loss of H1. Additionally, the $M_1 =$ 8.3 nucleosomes/10 nm measured here for chicken

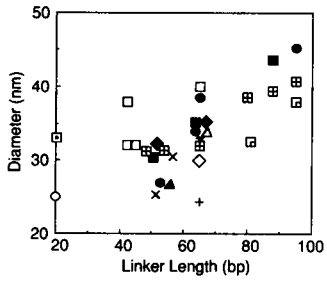

FIGURE 9 Diameters of chromatin higher-order structure measured by x-ray and neutron scattering as a function of linker lengths. Solid symbols indicate R_c determined by Guinier analyses; hollow symbols indicate the less reliable, model-dependent, analyses of higher-angle diffraction features. R_c was converted to diameter by multiplying by $2\sqrt{2}$. Fiber length is in units of nucleosomes. Ionic strengths have been calculated from the original references. The numbers in parentheses are the concentrations of divalent cations, when present. A positive symbol in the H1 column indicates that the presence of significant amounts of H1 was noted in the original reference. A negative symbol indicates that measurement was not reported.

Symbol	Ionic strength	Length	H1	Reference
▲	15 mM (2 mM Mg)	50	+	Suau et al., 1979
×	100–150 mM	—	–	Notbohm et al., 1979; Brust and Harbers, 1981
◆	10 mM (12 mM Mg)	50	–	Dunn et al., 1986
●	80–125mM	70–170	+	Bordas et al. 1986; Koch et al., 1988
+	150 mM	50	–	Greulich et al., 1987
✳	130 mM	105	–	Gerchman and Ramakrishnan, 1987
■	120 mM	130–200	+	this paper
△	15 mM (2 mM Mg)	50	+	Suau et al., 1979
□	43–110 mM (3–5 mM Mg)	nuclei	+	Langmore and Paulson, 1983
◇	85 mM	23	–	Lasters et al., 1985
⊞	120 mM	nuclei	–	Williams et al., 1986
○	20 mM (4 mM Mg)	nuclei	–	Koch et al., 1987
⊡	23 mM (5 mM Mg)	nuclei	–	Lowary and Widom, 1989
□	120 mM	nuclei	–	Williams (1989) measurements from *Sipunculoid* erythrocytes (81 bp) and white blood cells (95 bp)

erythrocyte chromatin is in good agreement with values of 8 nucleosomes/10 nm reported by Dunn et al. (1986). On the other hand, 6 nucleosomes/10 nm was reported by Gerchman and Ramakrishnan (1987) by neutron diffraction, and 4 nucleosomes/10 nm by x-ray scattering at the monovalent ion concentration of EB (Bordas et al., 1986*a*; Koch et al., 1987), possibly reflecting H1 loss during the dialysis or sedimentation steps. Another possibility is that the much higher concentrations used in the other x-ray studies led to preferential precipitation of the more compacted fibers, leaving the less condensed fibers in solution.

Nucleosome spacing with chromatin is conserved

Given the highly conserved sequence of the core histones and the conserved three-dimensional structure of the nucleosome core, it is likely that the interactions between nucleosomes within chromatin are conserved. The R_c measurements (Table 2) indicate a 30% difference in fiber diameter between *Necturus* erythrocyte and *Thyone* sperm chromatin, leading to a much larger volume to be occupied by the nucleosomes. Assuming an axial repeat of 13 nm (Williams et al., 1986), experimental values for R_c and M_l, and placement of the nucleosome cores at the edge of the fibers, the internucleosomal distances along the helical gyres can be calculated. The center-to-center separation of nucleosomes in a double-helical model would be 7.5 nm for *Necturus* and 7.2 nm for *Thyone*. In a single-helical model the distances would be 7.2 nm for *Necturus* and 7.0 nm for *Thyone*. The calculation suggests conservation of core particle interactions regardless of linker length.

Relevance to higher angle scattering

The R_c measurements help explain the scattering patterns from chromatin at high concentrations. The tissue-specific features at $s \approx 0.05$ nm^{-1} in the low angle spectra of living cells, nuclei, and concentrated gels at physiological salt has been interpreted as the first subsidiary maximum of the Fourier transform of chromatin cylinders of variable diameter (Langmore and Schutt, 1980; Langmore and Paulson, 1983; Williams et al., 1986; Bordas et al., 1986*a*; Koch et al., 1987). Diameter estimates based on that feature are 5–10% smaller than values obtained from R_c, but exhibit the same dependence on linker length (Fig. 9). This difference seems to represent a systematic error in curve fitting of the $s \approx 0.05$ nm^{-1} peak owing to particle–particle interference at the high chromatin concentrations in nuclei.

A peak at $s \approx 0.03$ nm^{-1}, observed when chromatin is condensed by multivalent cations, has been attributed directly to the side-by-side packing of the fibers (Langmore and Paulson, 1983; Widom and Klug, 1985; Koch et al., 1987). However, the estimates of chromatin fiber diameters based on the position of the packing reflection appear to be incorrectly large (Fig. 9), apparently due to substantial separation of the fibers. Use of this reflection led Langmore and Paulson (1983) and Lowary and Widom (1989) to systematically overestimate fiber diam-

eters (although still showing the correct dependence upon linker length).

The conserved nature of the higher angle diffraction features has been interpreted as being indicative of the conserved nature of nucleosome interaction within the fibers (Langmore and Paulson, 1983; Widom and Klug, 1985; Widom et al., 1985). Our values for R_c and M_1 support the hypothesis that the side-by-side packing of nucleosome cores within fibers is conserved. Oriented x-ray diffraction patterns (Richards and Pardon, 1970; Baldwin et al., 1978; Widom and Klug, 1985; Widom et al., 1985) and Fourier transforms of electron micrographs (Williams et al., 1986) also indicate that the helical repeat is conserved.

Comparison with electron microscopy studies of fiber diameter

The R_c values obtained here are consistent with solid cylinders of diameters 31, 34, and 45 nm for *Necturus,* chicken, and *Thyone* chromatin. Although R_c is very sensitive to the outer diameter of a fiber, it is relatively insensitive to internal structure. Creation of a 13-nm central hole in a 45-nm fiber would only change R_c by 5%. Thus, R_c should give a fairly reliable estimate of the diameter of chromatin fibers. The hypothesis that R_c can be used to accurately estimate outer diameter is strengthened by recent STEM results showing that the internal density of the fibers is relatively constant (Smith et al., 1990).

There have been relatively few quantitative microscopic investigations of chromatin structure. Objective image processing techniques allow small differences in population means to be measured, even with a heterogeneous structure such as chromatin. Measurements of negatively stained chromatin from *Necturus* and *Thyone* gave diameters of 30 and 38 nm (Williams et al., 1986). Analysis of freeze-dried *Necturus* and *Thyone* fibers gave diameters of 31 and 38 nm (Smith et al., 1990). The trend of fiber diameter with linker length was clearly exhibited, even if the absolute values are smaller than the x-ray values.

Recent measurements of frozen-hydrated chromatin yielded diameters of 32.0 nm for *Necturus,* and 43.5 nm for *Thyone,* in quantitative agreement with the 31 and 45 nm predicted from the R_c measurements presented here (Athey et al., 1990). These measurements are significant because they confirm that the structural parameters measured by electron microscopy of individual fibers chosen for their unaggregated appearance and uniform morphology are in agreement with those measured by x-ray scattering studies of bulk solutions.

There have been other measurements of fiber diameters from electron micrographs of negatively stained chromatin and embedded nuclei, but without the benefit of objective image processing or statistical analysis. Some researchers have consistently seen chromatin diameters of 30 nm from all tissues studied, including chicken erythrocytes (McGhee et al., 1980; Bates et al., 1981), ox neurons (19 bp linker) (Pearson et al., 1983), sea urchin sperm (95 bp linker) (Widom et al., 1985), and yeast (20 bp linker) (Widom, 1989). Because those studies are not substantiated by the x-ray results, we conclude that native chromatin was not maintained under the conditions employed in those microscopy studies or that the measurements were not sufficiently accurate to detect the differences. Zentgraf and Franke (1984) have measured 37, 28, and 26 nm for the diameters of sea urchin (95 bp linker), chicken erythrocyte (64 bp linker), and rat liver (54 bp linker) chromatin in embedded nuclei, showing a correlation between fiber diameter and linker length. Alegre and Subirana (1989) have also noted different diameters of embedded material, which they attributed to a dependence on linker length. Such measurements on embedded chromatin are fraught with artifacts, including extensive shrinkage, and total loss of internal structure, which has been documented by low-angle x-ray scattering from embedded chromatin and nuclei (Nicolaieff, 1967; Pooley et al., 1974; Langmore and Paulson, 1983).

Comparison with electron microscopy studies of mass per unit length

Our results agree with previous measurements of M_1 made by STEM. The 6.9 and 11.8 nucleosomes per 10 nm obtained by this study for *Necturus* and *Thyone* chromatin agree well with the values of 7.4 and 11.9 obtained for *Necturus* and *Thyone* by STEM (Williams et al., 1986). The value obtained for chicken erythrocyte chromatin agrees with a value of 8.7 nucleosomes/10 nm obtained by interpolation of the measurements of Woodcock et al. (1984) to the ionic strength of EB, and in fair agreement with the STEM results of 7.2 nucleosomes/10 nm of Gerchman and Ramakrishnan (1987). Both of these studies noted a high sensitivity of M_1 to the ionic strength, indicating progressive axial compaction as the ionic strength increased.

Comparison with hydrodynamic studies

Many hydrodynamic experiments have been performed to investigate the relationship between nucleosome packing density and linker length. Sedimentation experiments have been interpreted as being indicative of a conserved external geometry (Butler and Thomas, 1980;

Bates et al., 1981; Pearson et al., 1983). More recently, sedimentation coefficients of sea urchin sperm (94 bp linker) fibers have been shown to be 43% higher than for rat liver fibers (54 bp linker) also containing 80 nucleosomes (Thomas et al., 1986). This result was attributed to differences in fiber stability rather than external geometry.

Our measurements of R_c and M_1 suggest that the observed differences in sedimentation were the result of sea urchin fibers being shorter than the rat liver fibers of the same molecular weight. Williams (1989) has tested this hypothesis by predicting and measuring the sedimentation coefficients of *Thyone* and *Necturus* chromatin. Using theoretical predictions of sedimentation coefficients for solid cylinders (Harrison and Klug, 1966), experimental values for nucleosome molecular weights, diameters, and M_1 for *Thyone* and *Necturus* chromatin, Williams calculated that an 80-mer of the long-linker chromatin should sediment 30% faster than an 80-mer of the intermediate-linker chromatin. The predicted values agree fairly well with the results of Thomas et al. (1986). Without fixation, *Thyone* and *Necturus* sedimented at similar velocities (Williams, 1989). Unfortunately, reproducible sedimentation coefficients of native fibers could not be measured at the ionic strength of EB, due to the fact that successive centrifugations of the same samples yielded smaller values for the sedimentation coefficient of fibers having the same molecular weight. It is possible that this apparent unraveling of chromatin is due to partial depletion of H1. After fixation, 80-mers of *Thyone* sedimented 60% faster than 80-mers of *Necturus* chromatin. Unfortunately, the changes in internal structure and M_1 caused by fixation prevent interpretation of the sedimentation coefficients of fixed chromatin.

Dichroic relaxation experiments on fibers isolated from different tissues were interpreted as supporting a conserved fiber geometry (McGhee et al., 1983). The results presented here are in disagreement with those interpretations. There are many possibilities why the differences in secondary structure were not undetected in this dichroism study, including loss of H1 or distortion of the fibers by the high electric fields (Sen and Crothers, 1986; Dimitrov et al., 1988). The highly divergent results for dichroic ratios in the literature also make it difficult to draw reliable conclusions from any of the optical studies.

Implications for proposed chromatin structures

The proposed structures for chromatin are the solenoid, twisted-ribbon, and crossed-linker models. According to the solenoid model, an 11 nm nucleofilament is twisted into a single-start helix, with successive nucleosomes in contact. Proposed solenoid models (Finch and Klug, 1976; McGhee et al., 1983; Butler, 1984) have diameters of 30 nm, helical repeat of 11 nm, and mass per unit length of 5–6 nucleosomes/10 nm, independent of linker length. The measurements of R_c and M_1 (Fig. 9; Table 2) are inconsistent with the constant-diameter solenoid models.

Athey et al. (1990) have proposed a variable-diameter solid-solenoid model having helical parameters that agree with the linker-length dependence of fiber diameter and mass per unit length found in the present study. That model is also in agreement with the observation that the fibers are not hollow (Smith et al., 1990).

The twisted-ribbon models (Worcel et al., 1981; Woodcock et al., 1984) were proposed to account for the zig-zag nucleosome chains observed at low ionic strength. The structures are built by twisting the axis of a zig-zag ribbon of nucleosomes in a helical path. The Woodcock proposal that the linker DNA is oriented in the direction of the helical axis predicts that an increase in linker length would increase the helical repeat, reduce the mass per unit length, but not affect fiber diameter. This model is inconsistent with the observations that increases of linker length preserve the apparent helical repeat (Langmore and Paulson, 1983; Widom and Klug, 1985; Widom et al., 1985; Williams et al., 1986), increase the mass per unit length (Williams et al., 1986; and this paper), and increase the diameter (Williams et al., 1986; Koch et al., 1987; Smith et al., 1990; Athey et al., 1990; and this paper). The Worcel proposal (1981) that the linker is slightly inclined from the helical axis predicts that an increase in linker length would increase the helical pitch, reduce the mass per unit length, and only slightly increase the fiber diameter. Thus the Worcel model is also inconsistent with the data.

Cross-linker models (Staynov, 1983; Makarov et al., 1985; Williams et al., 1986; Bordas et al., 1986*b*) were also proposed to account for the zig-zag nucleosome chains observed at low ionic strength. The zig-zag ribbon of nucleosomes is twisted about the ribbon (and also the fiber) axis, such that the nucleosomes follow helical paths. The crossed-linker models can be built with one (Staynov, 1983), two (Williams et al., 1986), three (Markarov et al., 1985), or more (Bordas et al., 1986*b*) helical gyres, with the linker DNA crossing through the interior of the fiber as it connects nonadjacent nucleosomes. Calculations based on the left-handed double-helical crossed-linker model predict R_c of 10 and 15.2 nm, and M_1 of 7.9 and 11.8 nucleosomes/10 nm for *Necturus* and *Thyone* chromatin (Williams and Langmore, unpublished results). Measurements of R_c and M_1 (Table 1) are in support of the double-helical crossed-linker model for chromatin structure.

We would like to thank D. Rankert for help in manuscript preparation and electron microscopy; M. Smith and B. Athey for enlightening discussions; and D. Sneider for facilities and assistance at the Brookhaven High Flux Beam Reactor.

These studies were supported by National Institutes of Health GM27937 and DIR-8706052. Dr. Williams was funded by a Research Partners Fellowship from The University of Michigan.

Received for publication 10 September 1990 and in final form 20 Novermber 1990.

REFERENCES

Alegre, C., and J. A. Subirana. 1989. The diameter of chromatin fibers depends on linker length. *Chromosoma (Berl.)*. 98:77–80.

Athey, B. D., M. F. Smith, S. P. Williams, D. A. Rankert, and J. P. Langmore. 1990. The diameters of frozen-hydrated Thyone and Necturus chromatin fibers increase with DNA linker length: evidence in support of variable diameter models for chromatin. *J. Cell Biol.* 111:795–806.

Baldwin, J. P., B. G. Carpenter, H. Crespi, R. Hancock, J. K. Stephens, J.K. Simpson, E. M. Bradbury, and K. Ibel. 1978. Neutron-scattering studies of chromatin subunits in solution under a variety of contrast conditions. *J. Appl. Cryst.* 11:484–486.

Bates, D. L., P. J. G. Butler, E. G. Pearson, and J. O. Thomas. 1981. Stability of the higher-order structure of chicken-erythrocyte chromatin in solution. *Eur. J. Biochem.* 119:469–476.

Bernal, J. D., and I. Fanchuchen. 1941. X-ray and crystallographic studies of plant virus preparations. *J. Gen. Physiol.* 25:111–165.

Boedtker, H., and N. S. Simmons. 1957. The preparation and characterization of essentially uniform tobacco mosaic virus particles. *J. Am. Chem. Soc.* 80:2550–2556.

Bordas, J., L. Perez-Grau, M. H. J. Koch, M. C. Vega, and C. Nave. 1986*a*. The superstructure of chromatin and its condensation mechanism. I. Synchrotron radiation x-ray scattering results. *Eur. Biophys. J.* 13:157–173.

Bordas, J., L. Perez-Grau, M. H. J. Koch, M. C. Vega, and C. Nave. 1986*b*. The superstructure of chromatin and its condensation mechanism. II. Theoretical analysis of the x-ray scattering patterns and model calculations. *Eur. Biophys. J.* 13:175–185.

Brust, R., and E. Harbers. 1981. Structural investigations on isolated chromatin of higher-order organization. *Eur. J. Biochem.* 117:609–615.

Butler, P. J. G. 1984. A defined structure of the 30 nm chromatin fibre which accommodates different nucleosomal repeat length. *EMBO J.* 3:2599–2604.

Butler, P. J. G., and J. O. Thomas. 1980. Changes in chromatin folding in solution. *J. Mol. Biol.* 140:505–529.

Caron, F., and J. O. Thomas. 1981. Exchange of histone H1 between segments of chromatin. *J. Mol. Biol.* 146:513–537.

Caspar, D. L. D. 1963. Assembly and stability of the tobacco mosaic virus. *In* Advances in Protein Chemistry. C. B. Anfinson Jr., M. L. Anson, and J. T. Edsall, editors. Academic Press, Inc., NY. 18:37–121.

Dimitrov, S. I., I. V. Smirnov, and V. Makarov. 1988. Optical anisotropy of chromatin. Flow linear dichroism and electric dichroism studies. *J. Biomol. Struct. Dyn.* 2:1135–1148.

Dubochet, J., M. Adrian, J. Chang, J.-C. Homo, J. Lepault, A. W. McDowall, and P. Schultz. 1988. Cryo-electron microscopy of vitrified specimens. *Q. Rev. Biophys.* 21:129–228.

Dunn, S. P., J. P. Baldwin, L. Wyns, S. Muyldermans, I. Lasters, G. A. Poland, D. Z. Staynov, H. W. E. Rattle, and M. J. Wood. 1986. Neutron scattering of chromatin multinuleosomes. *Physica.* 136B: 265–267.

Finch, J. T., and A. Klug. 1976. Solenoidal model for superstructure in chromatin. *Proc. Natl. Acad. Sci. USA.* 73:1897–1901.

Gerchman, S. E., and V. Ramakrishnan. 1987. Chromatin higher-order structure studied by neutron scattering and scanning transmission electron microscopy. *Proc. Natl. Acad. Sci. USA.* 84:7802–7806.

Greulich, K. O., J. Ausio, and H. Eisenberg. 1985. Nucleosome core particle structure and structural changes in solution. *J. Mol. Biol.* 185:167–173.

Greulich, K. O., E. Wachtel, J. Ausio, D. Seger, and H. Eisenberg. 1987. Transition of chromatin from the "10 nm" lower order structure, to the "30 nm" higher order structure as followed by low angle x-ray scattering. *J. Mol. Biol.* 193:709–721.

Guinier, A., and G. Fournet. 1955. Small Angle X-ray Scattering. John Wiley & Sons, New York. 20–48.

Harrison, B. D., and A. Klug. 1966. Relation between length and sedimentation coefficient for particles of tobacco rattle viruses. *Virology.* 30:738–740.

Hartt, J., and R. Mendelson. 1980. X-ray scattering of f-actin and myosin subfragment 1 complex. *Fed. Proc.* 39:1728.

Koch, M. H. J., M. C. Vega, Z. Sayers, and A. M. Michon. 1987. The superstructure of chromatin and its condensation properties. III. Effect of monovalent and divalent cations x-ray solution scattering and hydrodynamic studies. *Eur. Biophys. J.* 14:307–319.

Koch, M. H. J., Z. Sayers, A. M. Michon, R. Marquet, C. Houssier, and J. Willfuhr. 1988. The superstructure of chromatin and its condensation mechanism. V. Effect of linker length, condensation by multivalent cations, solubility, and electric dichroism properties. *Eur. Biophys. J.* 16:177–185.

Kratky, O. 1964. X-ray small-angle scattering with substances of biological interest in diluted solutions. *Prog. Bioph. Mol. Biol.* 13:105–173.

Lake, J. A. 1967. An iterative method of slit correcting small angle x-ray data. *Acta Crystallogr.* 23:191–194.

Langmore, J. P., and C. Schutt. 1980. The higher order structure of chicken erythrocyte chromosomes *in vivo*. *Nature (Lond.)*. 288:620–622; 291:359–360.

Langmore, J. P., and J. R. Paulson. 1983. Low angle x-ray diffraction studies of chromatin structure *in vivo* and in isolated nuclei and metaphase chromosomes. *J. Cell Biol.* 96:1120–1131.

Lasters, I., L. Wyns, S. Muyldermans, J. P. Baldwin, G. A. Poland, and C. Nave. 1985. Scatter analysis of discrete-sized chromatin fragments favours a cylindrical organization. *Eur. J. Biochem.* 151:283–289.

Lowary, P. T., and J. Widom. 1989. Higher-order structure of Saccharomyces cerevisiae chromatin. *Proc. Natl. Acad. Sci. USA.* 86:8266–8270.

Luzatti, V. 1960. Interpretation des mesures absolues de diffusion centrale des rayons X on collimation ponctuelle ou lineare: solutions de particules globulaires et de batonnets. *Acta Crystallogr.* 13:939–945.

Makarov, V., S. Dimitrov, V. Smirnov, and I. Pashev. 1985. A triple helix model for the structure of chromatin fiber *FEBS (Fed. Eur. Biochem. Soc.) Lett.* 181:357–361.

Malmon, A. G. 1957. Small-angle x-ray scattering functions for ellipsoids of revolution and right circular cylinders. *Acta Crystallogr.* 10:639–642.

Markham, R., J. H. Hitchborn, G. J. Hills, and S. Frey. 1964. The anatomy of the tobacco mosaic virus. *Virology.* 22:342–359.

McGhee, J. D., D. C. Rao, E. Charney, and G. Felsenfeld. 1980. Orientation of the nucleosome within the higher order structure of chromatin. *Cell.* 22:87–96.

McGhee, J. D., J. M. Nickol, G. Felsenfeld, and D. C. Rau. 1983. Higher order structure of chromatin: orientation of nucleosomes within the 30 nm chromatin solenoid is independent of species and spacer length. *Cell.* 33:831–841.

Neuhoff, V., N. Arold, D. Taube, and W. Ehrhardt. 1988. Improved staining of proteins in polyacrylamide gels including isoelectric focusing gels with clear background at nanogram sensitivity using coomassie brilliant blue G-250 and R-250. *Electrophoresis.* 9:255–262.

Nicolaieff, A. 1967. Small Angle X-Ray Scattering. H. Brumberger, editor. Gordon and Breach, New York. 221–241.

Notbohm, H., H. Hollandt, J. Meissner, and E. Harbers. 1979. Low angle x-ray scattering studies of chromatin in different solvents: analysis by computer simulated scattering curves. *Int. J. Biol. Macromol.* 1:180–184.

Pearson, E. C., P. J. G. Butler, and J. O. Thomas. 1983. Higher-order structure of nucleosome oligomers from short-repeat chromatin. *EMBO J.* 2:1367–1372.

Pooley, A. S., J. F. Pardon, and B. M. Richards. 1974. The relation between the unit thread of chromosomes and isolated nucleohistone. *J. Mol. Biol.* 85:533–549.

Richards, B. M., and J. P. Pardon. 1970. The molecular structure of nucleohistone (DNH). *Exp. Cell Res.* 62:184–196.

Richmond, T. J., J. T. Finch, B. Rushton, D. Rhodes, and A. Klug. 1984. Structure of the nucleosome core particle at 7 Å resolution. *Nature (Lond.).* 311:532–537.

Sen, D., and D. M. Crothers. 1986. Condensation of chromatin: role of multivalent cations. *Biochemistry.* 25:1495–1503.

Smith, M. F., B. D. Athey, S. P. Williams, and J. P Langmore. 1990. Radial density distribution chromatin: evidence that chromatin fibers have solid cores. *J. Cell Biol.* 110:245–254.

Staynov, D. Z. 1983. Possible nucleosome arrangements in the higher-order structure of chromatin. *Int. J. Biol. Macromol.* 5:3–9.

Suau, P., E. M. Bradbury, and J. P. Baldwin. 1979. Higher order structures of chromatin in solution. *Eur. J. Biochem.* 97:593–602.

Thoma, F., Th. Koller, and A. Klug. 1979. Involvement of histone H1 in the organization of the nucleosome and of the salt-dependent superstructures of chromatin. *J. Cell Biol.* 83:403–427.

Thomas, J. O., and C. Rees. 1983. Exchange of histones H1 and H5 between chromatin fragments: a preference of H5 for higher-order structures. *Eur. J. Biochem.* 134:109–115.

Thomas, J. O., C. Rees, and P. J. G. Butler. 1986. Salt-induced folding of sea urchin chromatin. *Eur. J. Biochem.* 154:343–348.

van Holde, K. E. 1989. Chromatin. Springer-Verlag, New York. 292–303.

Wang, S. W., A. J. Robins, R. d'Andrea, and J. R. Wells. 1985. Inverted duplication of histone genes in chicken and disposition of regulatory sequences. *Nucleic Acids Res.* 13:1369–1387.

Widom, J., and A. Klug. 1985. Structure of the 300 Å chromatin filament: x-ray diffraction from oriented samples. *Cell.* 43:207–213.

Widom, J., J. T. Finch, and J. O. Thomas. 1985. Higher-order structure of long repeat chromatin. *EMBO J.* 4:3189–3194.

Widom, J. 1989. Toward a unified model of chromatin folding. *Annu. Rev. Biophys. Chem.* 18:365–395.

Williams, S. P. 1989. Characterization of Chromatin Structure in Nuclei and Solution. Ph.D. thesis. The University of Michigan, Ann Arbor, MI.

Williams, S. P., B. D. Athey, L. J. Muglia, R. S. Schappe, A. H. Glough, and J. P. Langmore. 1986. Chromatin fibers are left-handed double-helices with diameter and mass per unit length that depend on linker length. *Biophys. J.* 49:233–248.

Woodcock, C. L. F., L.-L. Y. Frado, and J. B. Rattner. 1984. The higher order structure of chromatin: evidence for a helical ribbon arrangement. *J. Cell Biol.* 99:42–52.

Worcel, A., S. Strogatz, and D. Riley. 1981. Structure of chromatin and the linking number of DNA. *Proc. Natl. Acad. Sci. USA.* 78:1461–1465.

Zentgraf, H., and W. W. Franke. 1984. Differences of supranucleosomal organization in different kinds of chromatin: cell type-specific globular subunits containing different numbers of nucleosomes. *J. Cell Biol.* 99:272–286.